RADC-TDR-64-38
FINAL REPORT

32-P $1.00

NANOSECOND PULSE BREAKDOWN IN GASES

TECHNICAL DOCUMENTARY REPORT NO. RADC-TDR-64-38

March 1964

Techniques Branch
Rome Air Development Center
Research and Technology Division
Air Force Systems Command
Griffiss Air Force Base, New York

Project No. 4506, Task No. 450603

(Prepared under Contract No. AF30(602)-2779 by Space Sciences, Inc., 301 Bear Hill Rd., Waltham, Mass. Authors: P. Felsenthal and J.M. Proud)

DDC AVAILABILITY NOTICE

Qualified requesters may obtain copies from the Defense Documentation Center (TISIR), Cameron Station, Alexandria, Va., 22314.

Releasable to OTS.

LEGAL NOTICE

When US Government drawings, specifications, or other data are used for any purpose other than a definitely related government procurement operation, the government thereby incurs no responsibility nor any obligation whatsoever; and the fact that the government may have formulated, furnished, or in any way supplied the said drawings, specifications, or other data is not to be regarded by implication or otherwise, as in any manner licensing the holder or any other person or corporation, or conveying any rights or permission to manufacture, use, or sell any patented invention that may in any way be related thereto.

DISPOSITION NOTICE

Do not return this copy. Retain or destroy.

Key Words: Pulse compression; gas discharger; electric discharger; dielectric properties.

ABSTRACT

It is shown analytically that under certain conditions pulsed DC and pulsed microwave breakdown are directly comparable. A pulsed DC experimental system to measure breakdown over a wide range of applied voltage, gas pressure and gap distance has been used to measure formative time in air helium and nitrogen. The results when compared with the theoretical predictions of breakdown confirm the utility of the theory in describing breakdown within the imposed limits. The accuracy and extent of the present measurements materially extend the present range of pulsed microwave breakdown data.

PUBLICATION REVIEW

This report has been reviewed and is approved. For further technical information on this project, contact Ronald C. Blackall, EMATP, Ext. 23200.

Approved: Ronald C Blackall
RONALD C. BLACKALL
A2/c., USAF
Project Engineer

Approved: Arthur J. Frohlich
ARTHUR J. FROHLICH
Ch, Techniques Branch
Surveillance & Control Division

FOR THE COMMANDER: Fred J Desmond
for IRVING J. GABELMAN
Chief, Advanced Studies Group

EVALUATION

1. This work is part of an RADC program aimed at determining the feasibility of utilizing nanosecond pulses to provide superior range resolution in long range radar. Interest has been confined to pulse durations shorter than twenty nanoseconds, which corresponds to range resolution better than ten feet, and peak powers in excess of one thousand megawatts. The objective of this contract was to gather useful "video" nanosecond pulse breakdown data on selected gases that might be used in such a radar.

2. The experimental technique utilizes a triggered spark gap to discharge a length of transmission line. This system generates pulses with rise times of 0.25 to 1.0 nanoseconds and amplitudes of 4 to 30 kilovolts. Air, helium and nitrogen have been tested and the results are in close agreement with theory. A contract extension is being negotiated in which additional gases will be tested using the existing equipments.

3. Complementary work is being done at Braddock, Dunn and McDonald, El Paso, Texas and at Microwave Associates, Burlington, Mass. Braddock, Dunn and McDonald, under Contract AF30(602)-2781 entitled "Nanosecond Pulse Breakdown Initiation and Growth" is studying breakdown initiation and the effects of surface conditions on breakdown. Microwave Assoc., under Contract AF30(602)-2782 entitled "Nanosecond Pulse Breakdown Study" is investigating breakdown at microwave frequencies with nanosecond pulses.

Ronald C. Blackall

RONALD C. BLACKALL
A2/c., USAF
Project Engineer

TABLE OF CONTENTS

TABLE OF FIGURES

1. Introduction

This report summarizes the results of a one year program to continue the investigation of certain aspects of gaseous breakdown. Emphasis has been placed on the study of the formative time of breakdown for high voltage pulses. The underlying purpose of the program has been to achieve an understanding of gaseous breakdown phenomena for use in the design of very high peak power, high resolution radar systems.

This year's effort was directed primarily toward experimental measurement of the nanosecond breakdown parameters of air, helium and nitrogen. The experimental results have been compared with the breakdown theory developed earlier in the program. The close agreement between experiment and theory has indicated the validity of the theory and the utility of the experimental method.

The significance of this finding lies in the fact that data obtained by DC pulses are immediately applicable to the microwave breakdown case. This is the result of carefully limiting the pulse breakdown theory and experiments to a breakdown regime controlled by gas processes alone as is true of the diffusion theory of microwave breakdown. The relative convenience of the DC technique means that single pulse experiments may be easily carried out over a wider range of parameters than possible by a high power microwave technique.

In the discussion that follows a brief review of the breakdown theory presented earlier (Ref. 1) is given. This is followed by a description of the experimental apparatus and the techniques used in obtaining data. A detailed review of the experimental results for each gas is followed by a summary of the principal results of the program.

2. Theory

In the original investigations of Townsend and coworkers high voltage breakdown theory was complicated by the necessity of taking into account electrode processes as well as gas processes. Not until the advent of high power radio frequency and microwave sources was it possible to have a true electrodeless discharge. The development of the diffusion theory of breakdown to describe high frequency breakdown unified a number of unrelated experimental results by describing breakdown, within certain limits, in terms of gas processes alone.

In the work described here this simplification of the breakdown problem has been applied to the formative time for breakdown in the DC case. In what follows we show the limits to be applied to formative time measurements in order to relate the results to the diffusion theory. Further, we obtain the equations describing formative times for these conditions and show how our results may be applied to the description of pulsed microwave breakdown. In order to establish the appropriate limits it is assumed that the experiment takes place between infinite parallel plates located distance d apart. One electrode is illuminated with ultraviolet light and serves as an electron source for the gap. A voltage pulse of V volts and zero rise time is applied to an electrode. The gas in the gap at pressure P now takes a finite time τ before it begins to conduct appreciable currents. Analytically it is found that the appropriate set of variables to describe the formative time for the above conditions are $P\tau$ (mm Hg-sec), E/P (volts/cm-mm Hg), where V/d = E and $P\Lambda$ (mm Hg-cm), where Λ is the characteristic diffusion length. For infinite parallel plates $\Lambda = d/\pi$.

In order to describe the growth of breakdown in terms of gas processes it is clear that the time scale must be such as to prevent interaction of electrons or ions with the electrodes. For instance, the electrons formed at the cathode may drift across the gap, strike the anode and eject secondary electrons. Hence, if gas processes are to govern the formative time then the gap distance must be greater than the electron drift velocity times the formative time. Adopting the criteria that one half the gap distance be equal to or greater than the drift distance the Mobility Amplitude Limit may be written

$$P\Lambda \geq k\, E/P \cdot P\tau \cdot 2/\pi$$

where k is the proportionality constant relating drift velocity and E/P.

If the formative time is short compared to the time of propagation of the voltage pulse across the gap then uniform field conditions will not exist. Hence the Uniform Field Limit may be written approximately

$$P\tau \geq 10^{-10}\ P\Lambda$$

If the gap distance becomes comparable to an electron mean free path the description of electron behavior used in the theory is no longer valid. The Mean Free Path Limit is then

$$P\lambda \geq 1/P_c$$

where P_c is the probability of collision.

One further limit is imposed on the breakdown conditions. Breakdown is unlikely if the formative time is less than the average time between collisions, i.e. the Collision Frequency Limit is

$$P\tau \geq P/\nu_c$$

where ν_c is the collision frequency.

These four limits are analogous to the limits derived for the diffusion theory of microwave breakdown and may be plotted on the $P\lambda$, $P\tau$ plane (Ref. 2). The derivation of the expression for formative time is also closely analogous to the microwave case.

Within the limits defined above it is possible to write the differential equation governing the time rate of growth of breakdown

$$\frac{\partial n}{\partial t} = \nu_i n - \nu_a n + \nabla^2 (Dn) \qquad (1)$$

where n is the electron density, ν_i the ionization rate, ν_a the attachment rate and D the electron diffusion coefficient. For the plane parallel geometry of our experiments the above yields

$$\frac{\partial n}{\partial t} = \nu_i n - \nu_a n - \frac{D\pi^2 n}{d^2} \qquad (2)$$

For the parameters used in our experiment it may be shown that the diffusion loss is negligible compared to attachment loss for air.

Likewise, for the nonattaching gases, nitrogen and helium, for the range of E/P investigated, it may be shown that the diffusion loss may be neglected in our case. Eliminating the diffusion term and making use of the relationships

$$\nu_i = \alpha \bar{v} = \alpha \mu E$$

$$\nu_a = \beta \bar{v} = \beta \mu E \qquad (3)$$

$$\bar{v} = \mu E = k E/P$$

where α and β are the first ionization coefficient and the attachment coefficient respectively, $\bar{v}$ is the drift velocity and μ the mobility; Equation (2) becomes

$$P\tau = \frac{\ln n_b/n_o}{k E/P (\alpha/P - \beta/P)} \qquad (4)$$

where n_b is the breakdown electron density and n_o is the initial electron density. This equation now gives a relation between $P\tau$ and E/P depending only on gas parameters and a constant $\ln n_b/n_o$.

Equation (4) is plotted for the various gases tested in Figures 5, 8, and 11. As explained in Section 4, experimentally determined values of α and β are used. In all cases a ratio of $\ln n_b/n_o$ of 10^8 was utilized to facilitate a comparison of results with other reported breakdown research (Ref. 3).

In the derivation of single pulse microwave breakdown (Ref. 3), use is made of the identical differential equation (Equation 1) used here to describe breakdown. Furthermore, the solution of the equation is in terms of the variables $P\tau$ and E_e/P. Here E_e is the effective field defined to be equivalent to the DC field. Hence microwave pulse breakdown measurements and formative time measurements within the limits defined above may be directly compared.

3. Apparatus

The experimental apparatus is capable of measuring breakdown times in the regime described by the above theory. The apparatus allows a wide range of the parameter E/P to be examined, while maintaining time resolution of less than 0.3 nanoseconds. Gap distances and pressures may also be varied over a wide span of values.

Two functional capabilities underscore the apparatus design throughout. First, consideration had to be given to the high voltage capability of the overall pulse circuit, which must be capable of passing and switching nanosecond pulses of many kilovolts amplitude. Secondly, because of the short pulse duration, the frequency spectrum of the pulses generated extends from DC to the gigacycle range. Therefore, the entire apparatus is designed as a transmission line system with a frequency response spanning this spectrum.

The electrical system is similar to that developed by Fletcher (Ref. 4). It provides for the generation of pulses with the rise times of 0.25 to 1.0 ns with amplitudes of 4 to 30 kilovolts. It also provides an attenuated sample of the pulse for measurement of breakdown times, appropriate triggers and a source of ultraviolet light for illumination of the test gap. A schematic of the system is shown in Figure 1. The main pulse generator is a high pressure coaxial three ball gap used to discharge a 60 ns length of RG-17. The two outer balls may be moved axially relative to the fixed center ball. The gap is of tapered 52 ohm coaxial construction with a small pulse shaping condensor incorporated in the charging line side of the gap. Gas pressure and ball gap distance are adjusted to give proper operation at various cable charge voltages. Nitrogen or argon with pressures from 80 to 150 psi is used as the insulating gas.

The coaxial current viewing resistor is 0.212 ohm. The resistor output is passed through a 4 gc bandwidth coaxial pad of 6, 10 or 13 db and then to a 3 db power divider and a matching transformer for the 125 ohm oscilloscope deflection system. The other output of the power divider is used to trigger the oscilloscope. A Tektronix 519 oscilloscope with a deflection sensitivity of 9.8 v/cm and rise time of 0.29 nanoseconds is used to view the signals. With the aid of ASA 10,000 Polaroid film and an image reduction of 2:1 single trace photographs at 2 nanoseconds/cm may be obtained.

In addition to the current viewing resistor, the transmission line connecting the pulse generator and the test gap contain a 10 meg ohm resistor between the center and outer conductors to dissipate any net charge left on this portion of the system after the high voltage pulse has been applied to the test gap. A 50 ohm termination on the other side of the test gap provides a proper load for pulses transmitted through the gap when breakdown occurs.

The system trigger and ultraviolet illumination for the cathode are provided by the charged length of RG-8. A low voltage pulse is used to start the discharge of a ball-to-plane-to-point air gap. A first surface, 2.5 cm focal length mirror is used behind the plane-to-point discharge to increase the light output. The high voltage pulse from this discharge is used to trigger the pulse generator.

Two different test gaps have been used in the measurements reported here. Both gaps are basically the same tapered, 50 ohm coaxial construction. Polystyrene was used as the insulating material because of its low and uniform dissipation factor over the range of frequencies contained in the pulse. Both gaps have quartz windows for the admission of ultraviolet light to the cathode surface, ports for the admission of the test gases and pumping ports. Polished aluminum electrodes with Rogowski contours (Ref. 5) are used to provide uniform field conditions. The small gap is approximately 7.6 cm inside diameter with electrodes 3.5 cm diameter. The gap distance is adjustable by means of a 20 turns per inch thread. Gap distance of 0.13 to 2.0 centimeters are used. The large gap (Figure 2) is approximately 20.2 cm inside diameter with electrodes of 8.0 cm diameter. Fixed spacers are used to provide gap distances of 2.0, 4.0 and 6.0 centimeters. The maximum error in setting the gap distance is estimated to be less than 5%. A two stage mechanical pump with a zeolite trap is used to evacuate the test gap. Ultimate pressure of both gaps as measured on an Alphatron gauge is in the range of 1 to 2×10^{-3} mm Hg. During measurements the test gas is admitted through a variable leak, and the pumping speed reduced by a throttling valve. Thus a small flow of gas through the test gap is insured at all times. A standard mercury manometer is used as a check on the Alphatron gauge. Pressure measurements in the gap have an estimated accuracy of $\pm$ 2%.

The 20 kilovolt supply for the RG-8 line is fixed in output voltage so that adjustment of the air spark gap is unnecessary. Two separate supplies are used for charging the RG-17 line. A 0 to 13 kilovolt supply is used for low voltages and a 0 to 60 kilovolt supply for voltages from 16 to 30 kilovolts. Both supplies are 1% regulated and may be set to a given voltage with an average accuracy of $\pm$ 2%. When the RG-17 pulse cable is charged to a voltage V_o and discharged, the amplitude of the traveling wave is $V_o/2$. When the pulse reaches the test gap it is reflected back into the RG-17 coupling cable until such time as the test gap begins to conduct appreciable current. During the time that the traveling pulse is being reflected from the test gap electrode the voltage across the gap is V_o. Measurement of the traveling pulse amplitude seen through the current viewing resistor show it to be $V_o/2$ within 1%. Hence, we have assumed that the voltage to which the pulse cable is charged is the voltage applied to the test gap and that losses in the high pressure pulse generator are negligible. Rise time of the pulse depends on the particular voltage, the gas pressure in the pulse generator and the electrode distance. Rise times of 0.25 to 1.0 nanoseconds are observed. Figure 3 shows the rise time (0.8 nanoseconds) of a typical 13 KV pulse. Ringing and

overshoot are normally less then 10% of the average pulse amplitude. As may be seen the typical ringing frequency is the order of a few hundred megacycles. The exact amount of ringing not only varies with the voltage and gap setting but fluctuates slightly on a pulse to pulse basis. The rise time varies similarly.

The experimental apparatus has been in use for over one year. During this time it has proved reliable and relatively simple to adjust. The apparatus has not been degraded with use. Rise times presently obtained are identical to those obtained at the start of the program.

4. Results and Techniques

4.1. Measurement Technique

Measurements of the formative time of breakdown have been made in air, nitrogen and helium over a voltage range of 4 to 30 kilovolts, a pressure range of 1 to 760 mm Hg and an electrode gap width range of 0.13 to 6.0 cm. Results are discussed for each gas in later paragraphs in which a comparison of the formative time data with theory is given. The adherence to the validity conditions for the diffusion theory is also explored for each gas.

The meaningful interpretation of the breakdown data involves three experimental considerations which are applicable to all of the reported results. These include: the establishment of an operational criterion for the breakdown lag time based on the observed pulse shapes, the removal of the statistical variation from the lag time data and a consideration of departures from similarity for data obtained with differing combinations of the breakdown parameters.

Figure 3 shows a typical pulse waveform provided by the current viewing resistor placed in the transmission line near the test gap. As the traveling wave passes the resistor the rise time of the wavefront AB is seen. As the wave continues passing the resistor and arrives at the gap the level portion BC is observed. When the wavefront reflected from the anode reaches the CVR (C to D on the trace) the waves traveling in two opposite directions cancel each other for a time given by DE. If breakdown does not occur in the gap the reflected wave continues and the trace is as shown in DEF. If there are initial electrons present in the gas space so that breakdown takes place, the gap will begin to conduct after a short delay DE. When breakdown is fully formed, reflection from the gap ceases and the pulse height returns to its previous level as indicated by the portion GH.

For the purposes of this study the point E, indicating the onset of breakdown, is defined to correspond to a vertical deflection of one trace width above the base line of the trace. Further, we have measured formative time as the time between the instant the voltage reaches maximum on the anode (indicated by the point D in the observed pulse) and the time when the gap breaks down, E. Although these definitions are arbitrary, they are in accord with those used by other investigators.

The lag time DE is, in general, the sum of the formative and statistical lag times. The statistical delay time is caused by the finite rate of emission of electrons from the cathode surface and the statistical nature of the emission. Following the results of Strigel (Ref. 6) and the analysis suggested by von Laue (Ref. 7) the statistical time may be shown to obey an exponential distribution law. If the results of a number of measurements of the delay time for fixed voltage, pressure and gap distance are plotted on semilog axes with

appropriate variables the exponential nature of the distribution may be seen. The statistical delay is described by

$$n_t = n_o e^{-t/\sigma}$$

where n_t is the number of time lags greater than t, n_o is the total number of events and σ is the mean statistical lag. Hence a semilog plot of n_t/n_o versus t should be a straight line yielding a value for σ from the slope and a value for the minimum delay, or the formative time, from the intercept at $n_t/n_o = 1$. Figure 4 shows four typical plots of actual measurements. Such plots have been made for all data reported here where use is made, on the average, of 27 data points for the measured lag time.

By the methods referenced above it is possible to use the information regarding σ to estimate the rate of electron emission from the ultraviolet irradiation of the cathode surface. Based on typical observed values of σ from the data the photoemission current for this experiment is approximately 5×10^{-10} amperes.

According to the theory the formative time may be described in terms of the variables $P\bar{\tau}$ and E/P as in Equation (4). Similarity conditions should then apply in the sense that a particular value of E/P can be obtained from an unlimited number of combinations of the parameters: pressure, gap spacing and pulse voltage. Experimentally, departures are observed as illustrated in Figure 6. It is conjectured that the measured variations are due to the dependencies of the Townsend coefficient α/P and the drift velocity on absolute field strength as well as on the parameter E/P. Slight variations in gas composition at the different operating pressures may also play a role.

4.2. Breakdown Results in Air

The predictions of the formative time of breakdown have been made through the application of Equation (4), where empirical data for ionization and attachment coefficients and for the electron mobility have been employed. Ionization coefficient data are available from References 8 and 9 over a range of values of the parameter E/P up to 10^3 volts/cm-mm Hg. Attachment data from Reference 10 were used in the low portion of the E/P range where attachment is important. Drift velocity data obtained from Reference 8 extend to E/P values of 10^2 volts/cm-mm Hg. In order to formulate the breakdown predictions for higher values of E/P it has been necessary to employ an analytical expression for electron mobility based on the data for the lower range of E/P. The extrapolation then extends to E/P = 10^3 volts/cm-mm Hg to coincide with the range over which the ionization coefficient is known. For air, Equation (4) then becomes

$$P\tau = \frac{\ln n_b/n_o}{10^6 \left(\frac{7}{E/P} + 0.2\right) E/P \, (a/P - \beta/P)}$$

Use of the criterion for breakdown as prescribed in Section 2, i.e. $n_b/n_o = 10^8$, leads to the curve illustrated in Figure 5. The curve developed from the measured breakdown data is also included for comparison. In spite of the approximations made in the theoretical prediction, agreement is quite close over the entire range.

The experimental data are plotted in Figure 6 to illustrate their consistency with respect to the averaged curve. These data were collected over a nine month period without close control of humidity conditions, although air-conditioned room air of low relative humidity was employed throughout. The data illustrated were obtained over a range of gap distances from 0.13 to 6.0 cm, pulse voltages from 5 to 30 kilovolts and pressures from 1 to 760 mm Hg.

The data illustrated in Figure 6 were closely examined with regard to their position in the $P\tau$-$P\lambda$ plane relative to the limits of the diffusion theory. The location of data within this plane is illustrated in Figure 7. Only the Mobility Amplitude Limit, the Uniform Field Limit and the Collision Frequency Limit are included in the figure since the Mean Free Path Limit is off the scale used. The Mobility Amplitude Limit line for air is given by

$$P\lambda = 2/\pi \times 10^6 \, (7 + 0.2 \, E/P) \, P\tau$$

and is computed by an iterative procedure which employs averaged breakdown results. The dependence of this limit on breakdown data is reflected in the curvature of the line at $P\tau$ values less than 10^{-7} mm Hg-sec. It is seen from the figure that all reported data points are well within the diffusion theory limits.

The experimental breakdown data have been obtained for much higher values of E/P than can be treated by the theory due to the above noted lack of basic empirical data. As a result no comparison can be made for $E/P > 10^3$ volts/cm-mm Hg. The data are suggestive of an asymptotic approach to a minimum value of $P\tau$ in that region. It is quite plausible that this is brought about by an approach to conditions such that the collision frequency and ionization frequency are approximately equal.

4.3. Breakdown Results in Helium

The breakdown predictions for helium make use of the available mobility data (Ref. 11) which are given only over the range of the variable E/P from 0

to 5 volts/cm-mm Hg. Employing an analytical expression to extrapolate this information to higher values, the breakdown equation becomes

$$P\tau = \frac{\ln n_b/n_o}{7.6 \times 10^5 \, E/P \;\; \alpha/P}$$

Two available sets of ionization coefficient data are those obtained by von Engel and Steenbeck in 1932 (Ref. 12) and those published by Penning and Druyvesteyn in 1940 (Ref. 9). Predictions based on these two sets of ionization data are shown in Figure 8 along with the results of the present experiments. Agreement at the larger values of $P\tau$ is closest to predictions based on data from Reference 9, while at smaller values of $P\tau$ agreement is best with theory based on Reference 12 information. It is conjectured that this situation may be traced to similarities in gas purities between the referenced work and the present breakdown experiments. The breakdown measurements were carried out with impurities ranging from one part in 10^3 at values of E/P above 500 volts/cm-mm Hg to one part in 10^5 at lower values. The experimental variation in purity was due to the vacuum and continuous flow conditions which prevailed. The helium supply for the experiments had a purity of 99.996%.

The experimental breakdown points are shown in Figure 9 along with a curve of the average of the breakdown data. Values of the experimental parameters were varied over a range of pulse voltages from 5 to 25 kilovolts, pressures from 2 to 464 mm Hg and gap distances from 0.25 to 6.0 cm. Formative times were observed over a range from 0.4 to 18 nanoseconds.

The breakdown curve seems to have a distinct knee in the region of $P\tau$ between 10^{-7} and 10^{-8} mm Hg-sec. Because of the non-Maxwellian nature of the distribution of electron energies in helium for high E/P values (Ref. 8) it is difficult to pinpoint the cause for the changed slope. If it is the results of doubly ionized helium some simple spectroscopic investigations might provide insight.

The experimental data shown in Figure 9 are plotted on the $P\mathcal{A}$ - $P\tau$ plane in Figure 10. The Mobility Amplitude Limit line has been determined by an iterative process using the breakdown data and the following equation

$$P\mathcal{A} = 4.8 \times 10^5 \cdot E/P \cdot P\tau$$

The knee in the Mobility Amplitude Limit line is due to the change of slope of breakdown curve.

One interesting aspect of helium breakdown that has appeared in the experimental results is a reduction of breakdown pulse current for low pressures. For pressures of 1 mm Hg the equivalent gap impedance after the gap has broken

down is many hundreds of ohms as against a fraction of an ohm under normal circumstances.

4.4. Breakdown Results in Nitrogen

Theoretical estimates of breakdown in nitrogen have been made using drift velocity data obtained from References 8 and 13. The analytic expression to extend the limited range of drift velocity data to match the range of ionization coefficient data is identical to the expression found for air. Ionization data were obtained from Reference 8. The resulting breakdown equation

$$P\tau = \frac{\ln n_b/n_o}{10^6 \left(\frac{7}{E/P} + 0.2\right) E/P \; \alpha/P}$$

is plotted in Figure 11 . General agreement between theory and experiment may be seen.

The experimental data are plotted on the $P\tau$ - E/P plane in Figure 12 . The curve illustrates the average of the experimental points. Nitrogen used for these measurements had a purity of 99.78%. The experimental parameters were varied over pulse voltages of 4.0 to 20 kilovolts, gap distances of 0.13 to 6.0 cm and pressures of 1 to 780 mm Hg.

The experimental data as it appears on the $P\lambda$ - $P\tau$ plane is shown in Figure 13. The expression used for the iterative determination of the Mobility Amplitude Limit line is identical to that used for air. Where particular points lie close to the limit line a separate calculation of the minimum permissible $P\lambda$ value was made.

5. Conclusions

Results of the theory show that conditions exist where pulsed DC and pulsed microwave breakdown may be examined within the common framework of the diffusion theory. If pulsed experiments are carried out within the validity limits applicable to each, then the results obtained are equivalent. Physically, the application of the diffusion theory is tantamount to breakdown being governed by gas processes to the exclusion of wall or electrode effects. The present measurements have exploited DC techniques to obtain breakdown data over a range of breakdown parameters not fully accessible to microwave techniques.

Breakdown measurements have been completed for air, nitrogen and helium. In each case the agreement between the data and the diffusion theory prediction is quite close. This is true in spite of a lack of complete electron mobility data, which have been obtained by extrapolation of known values for purposes of predictions. The reliability of the reported data is quite high inasmuch as considerable attention has been given to the elimination of statistical lag components of the measured breakdown lag times and extensive efforts have been made to check similarity relations. Furthermore, each data point has been evaluated with respect to its adherence to the validity region for the diffusion theory.

Additional experimentation is planned to investigate the effects of known humidity conditions on air breakdown, the effects of a pulse repetition rate on breakdown and the pulse breakdown characteristics of several common insulating gases.

REFERENCES

1. J. M. Proud and P. Felsenthal, Nanosecond Breakdown in Gases, ~~RADC-TDR-62-617~~ Dielectric Strength Vol 17, 15 December 1962

2. S. C. Brown and A. D. McDonald, Phys. Rev. 76, 1629 (1949)

3. L. Gould and L. W. Roberts, J. Appl. Phys. 27, 1162 (1956)

4. R. C. Fletcher, Rev. Sci. Inst. 20, 861 (1949)

5. W. Rogowski, Arch. f. Elekt. 16, 73 (1926)

6. K. Strigel, Arch. f. Elekt. 26, 831 (1932)

7. M. von Laue, Ann. Phys. Lpz. 76, 261 (1925)

8. A. von Engel, Handbuch der Physik (Springer Verlag Berlin, 1956) XXI, p.504

9. M. J. Druyvesteyn and F. M. Penning, Rev. Mod. Phys. 12, 87 (1940)

10. M. A. Harrison and R. Geballe, Phys. Rev. 91, 1 (1953)

11. S. C. Brown, Basic Data of Plasma Physics (The Technology Press of M.I.T., 1959) p. 47

12. A. von Engel, M. Steenbeck, Elektrische Gasentladungen (J. Springer Verlag, 1932) I, p. 106

13. L. Colli and U. Facchini, Rev. Sci. Instr. 23, 39 (1952)

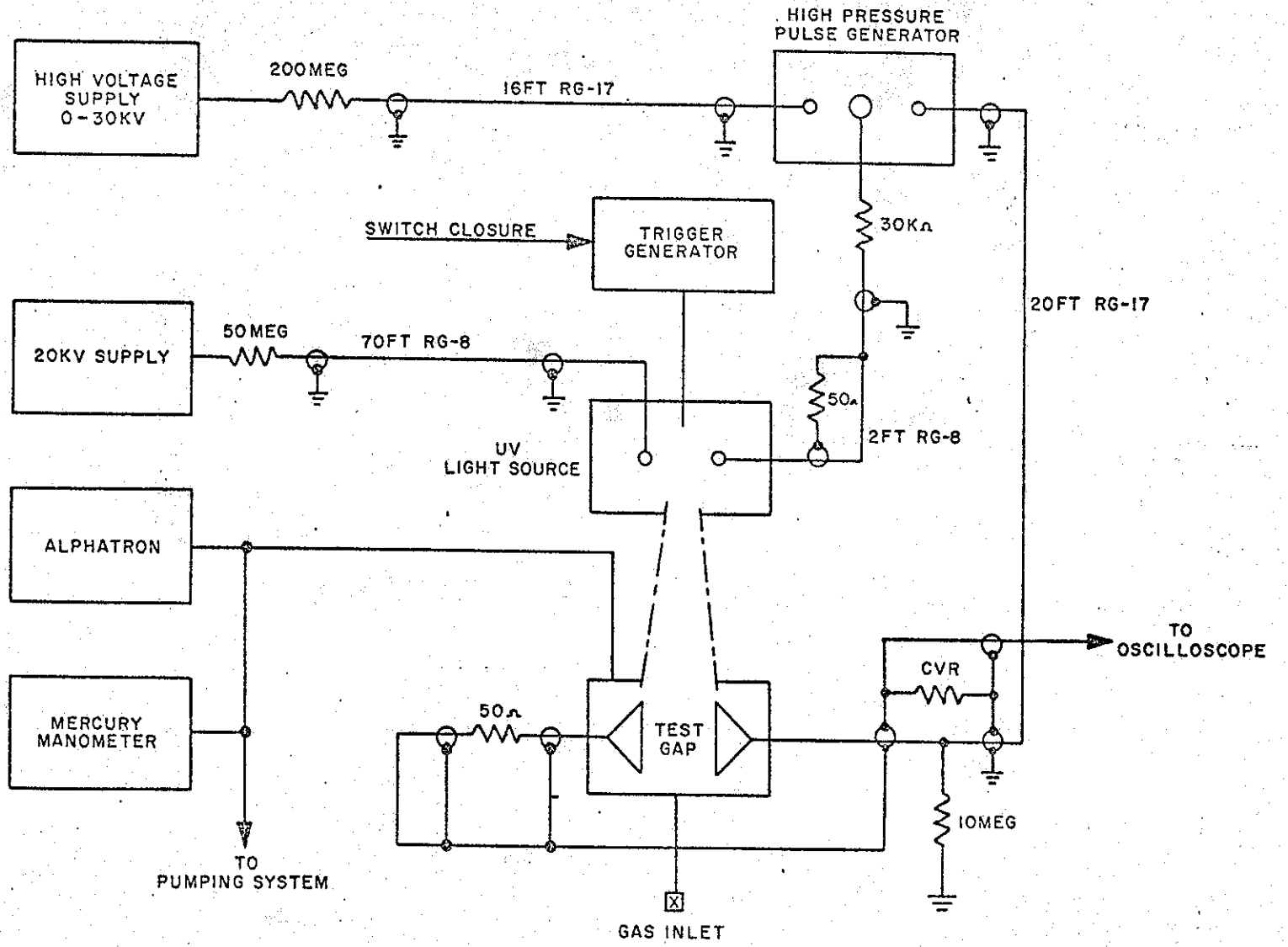

FIGURE 1. SCHEMATIC DIAGRAM OF EXPERIMENTAL APPARATUS.

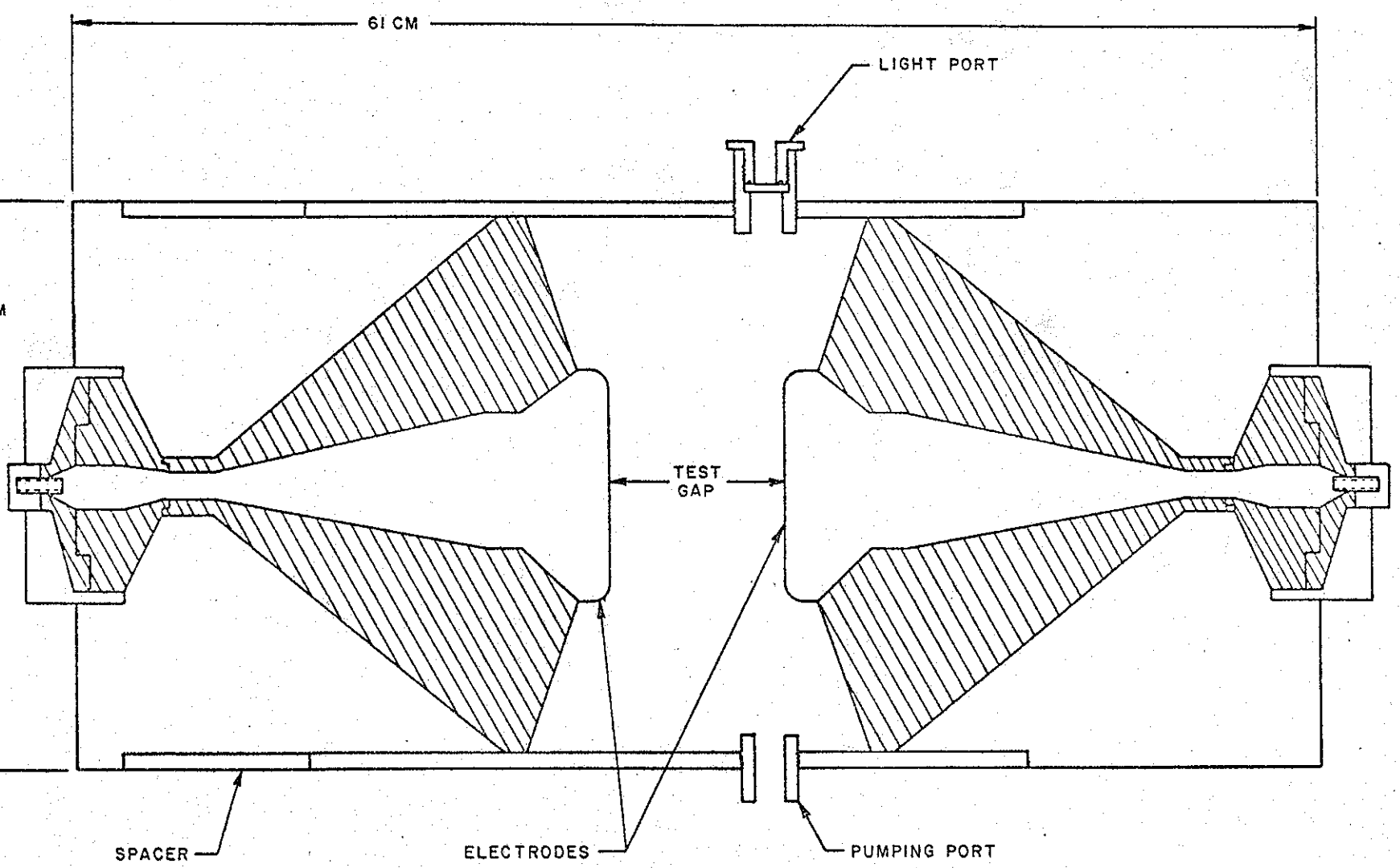

FIGURE 2. CROSS SECTION OF LARGE TEST GAP.

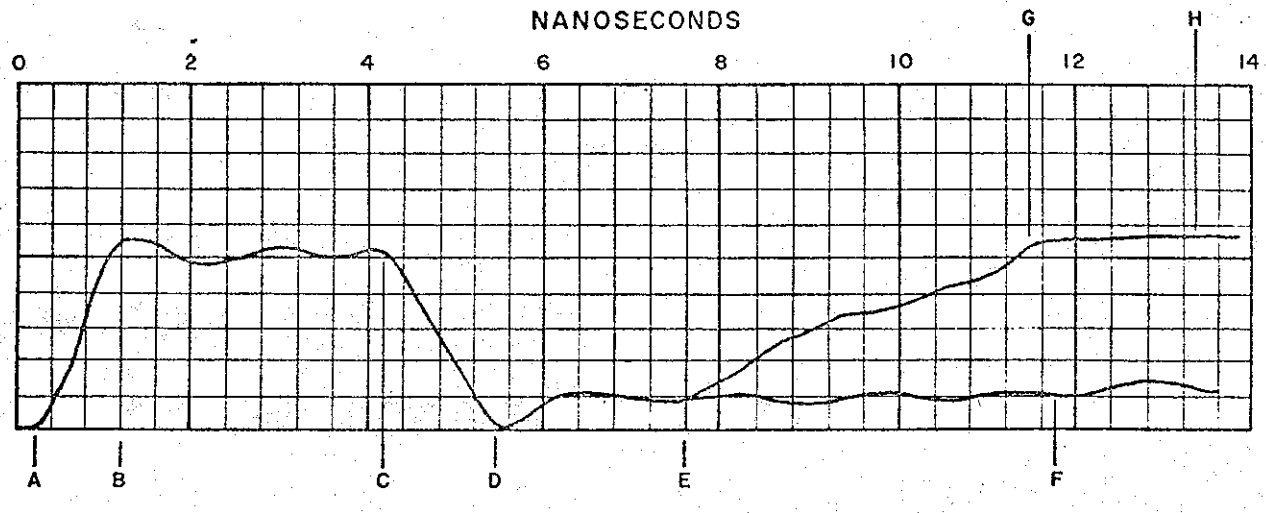

FIGURE 3. TYPICAL WAVEFORM.

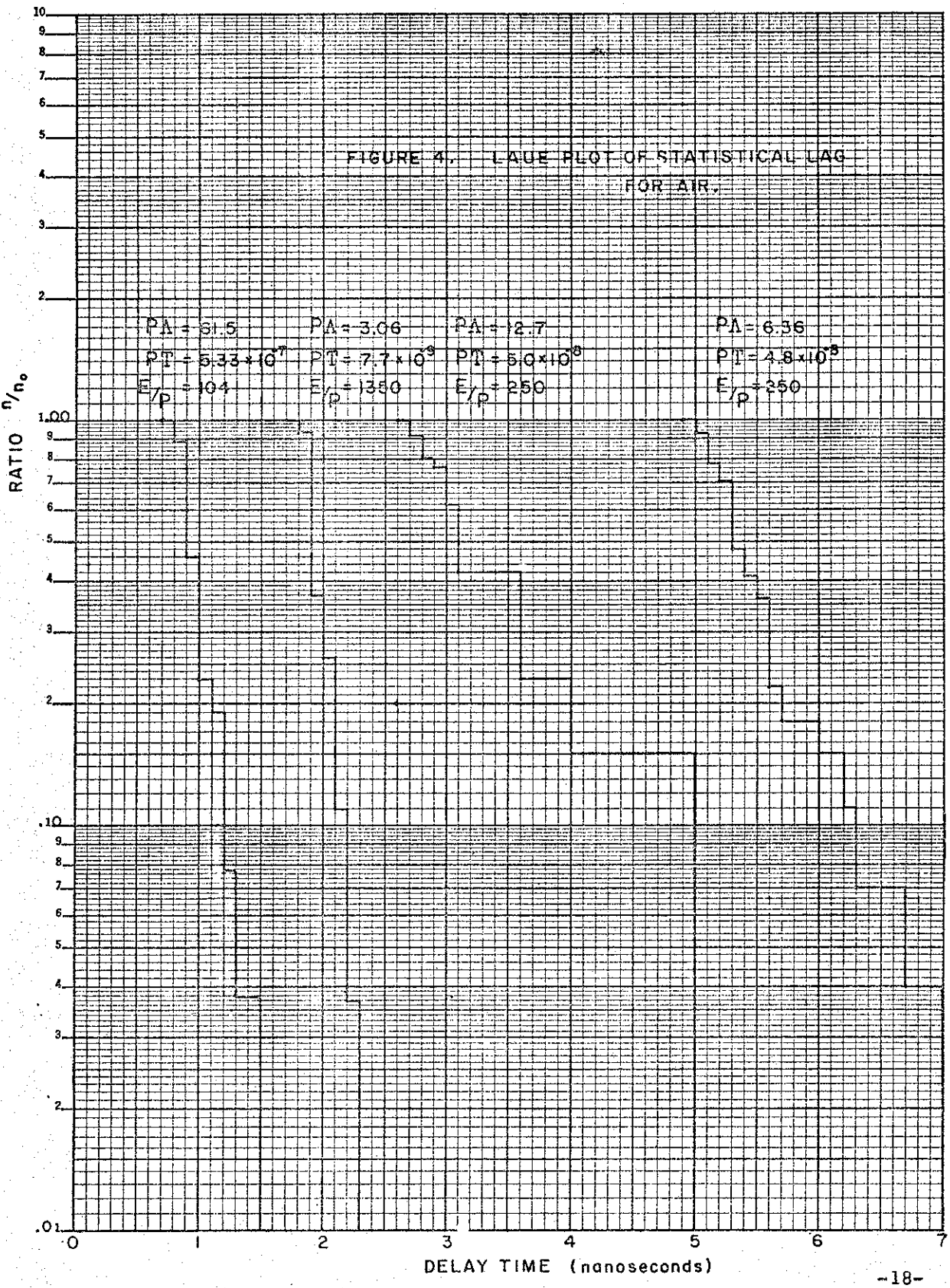

FIGURE 4. LAUE PLOT OF STATISTICAL LAG FOR AIR.

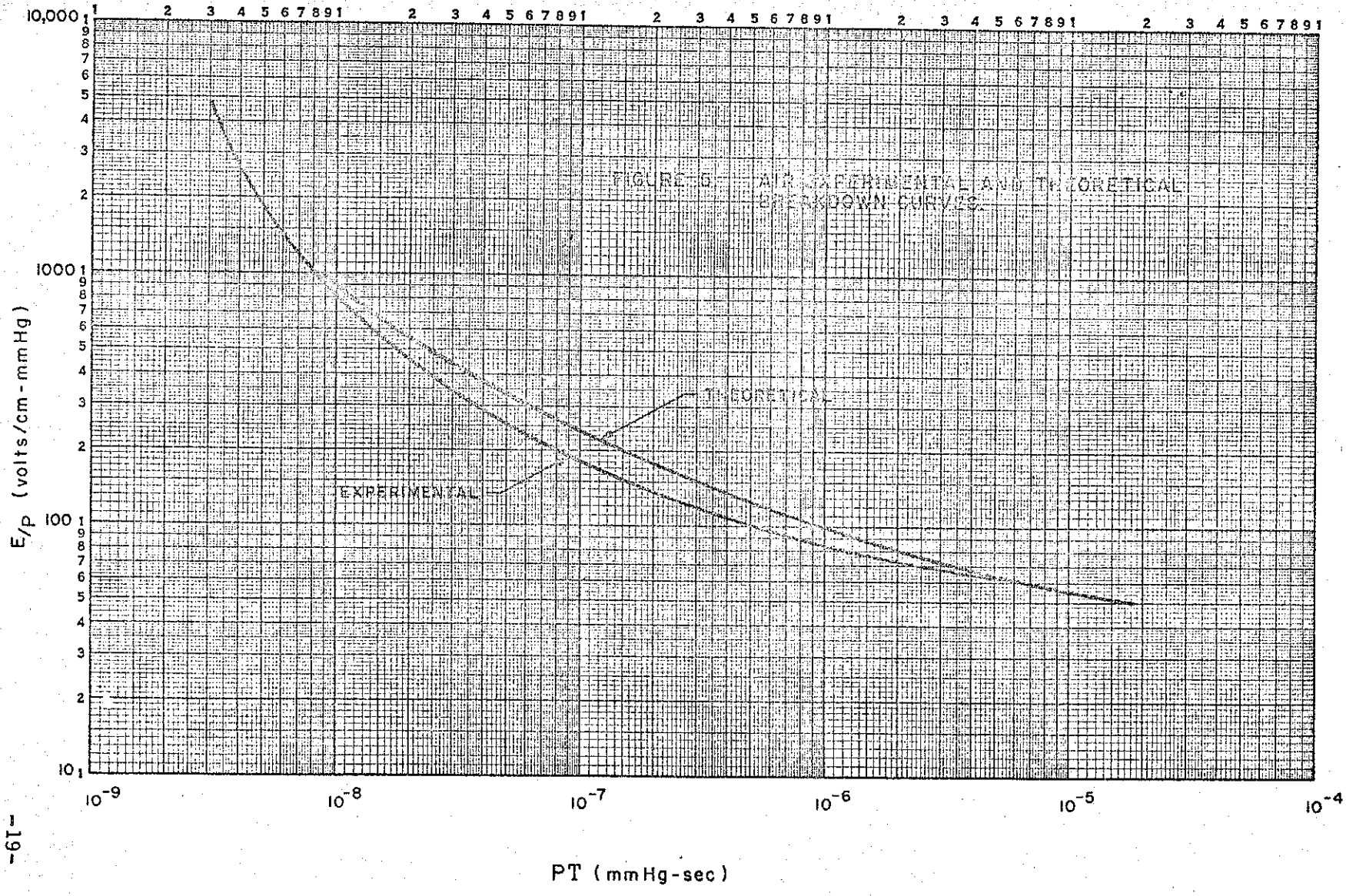

FIGURE 9. AIR EXPERIMENTAL AND THEORETICAL BREAKDOWN CURVES.

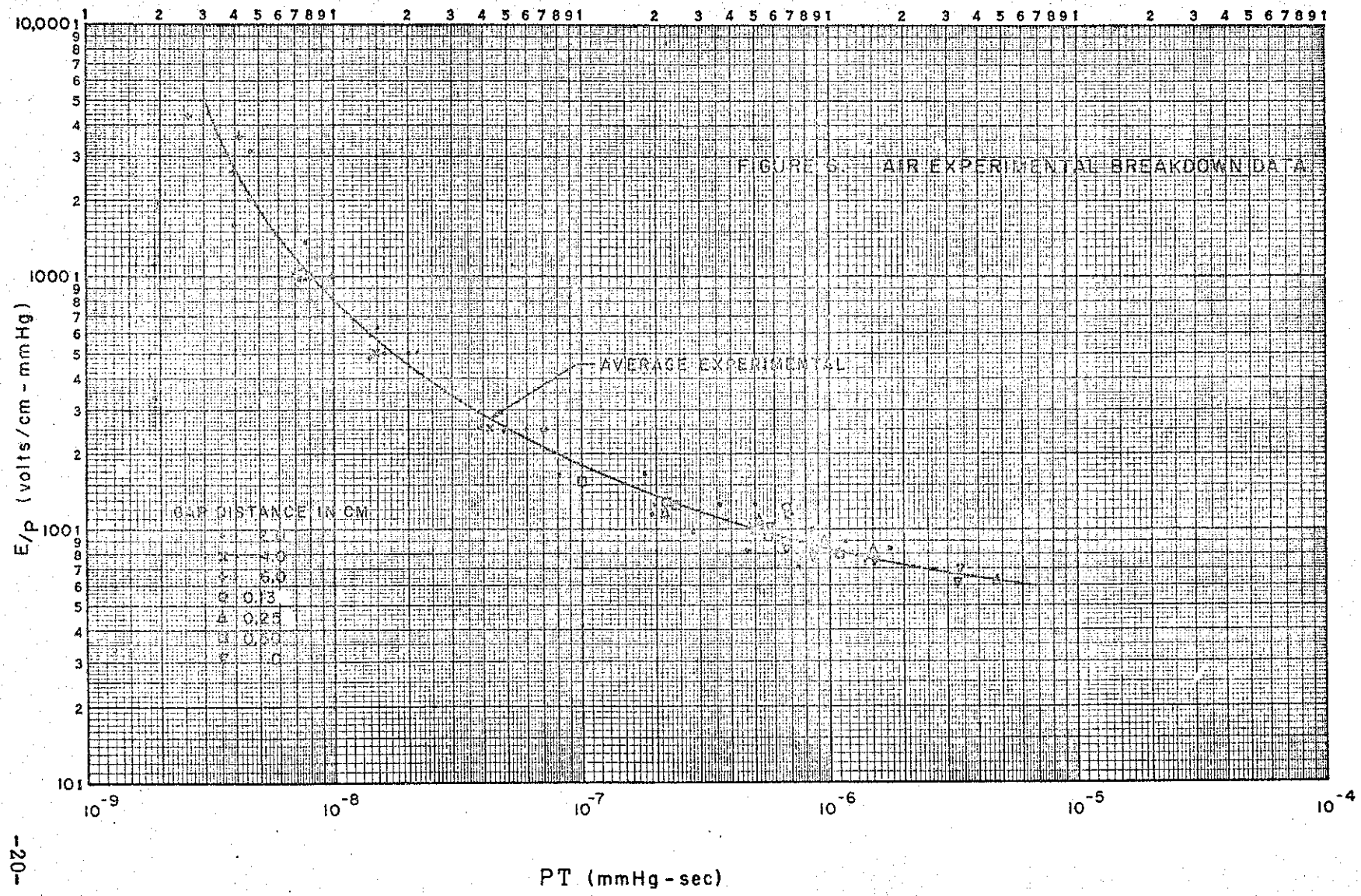

FIGURE 5. AIR EXPERIMENTAL BREAKDOWN DATA

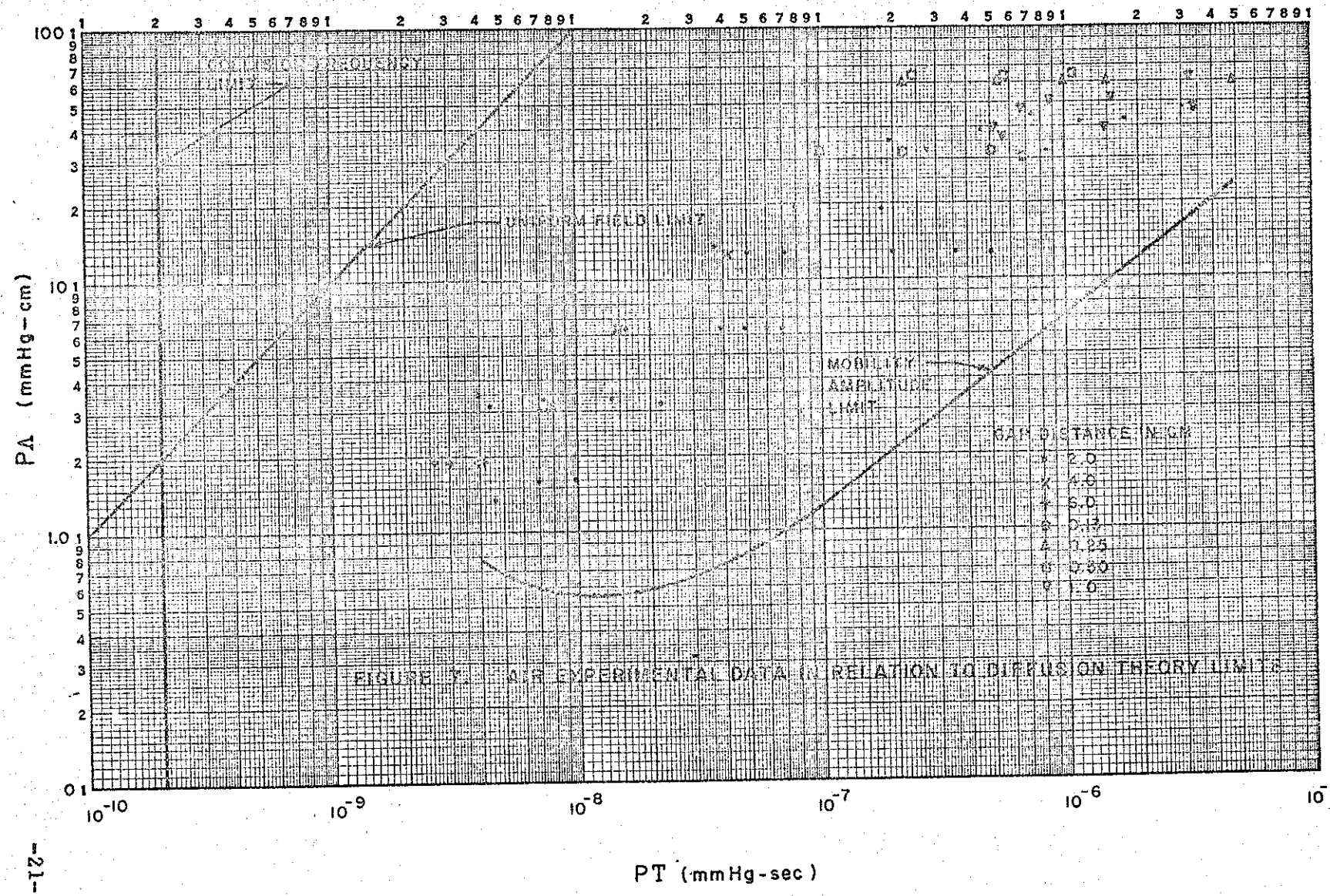

FIGURE 7. - AIR EXPERIMENTAL DATA IN RELATION TO DIFFUSION THEORY LIMITS

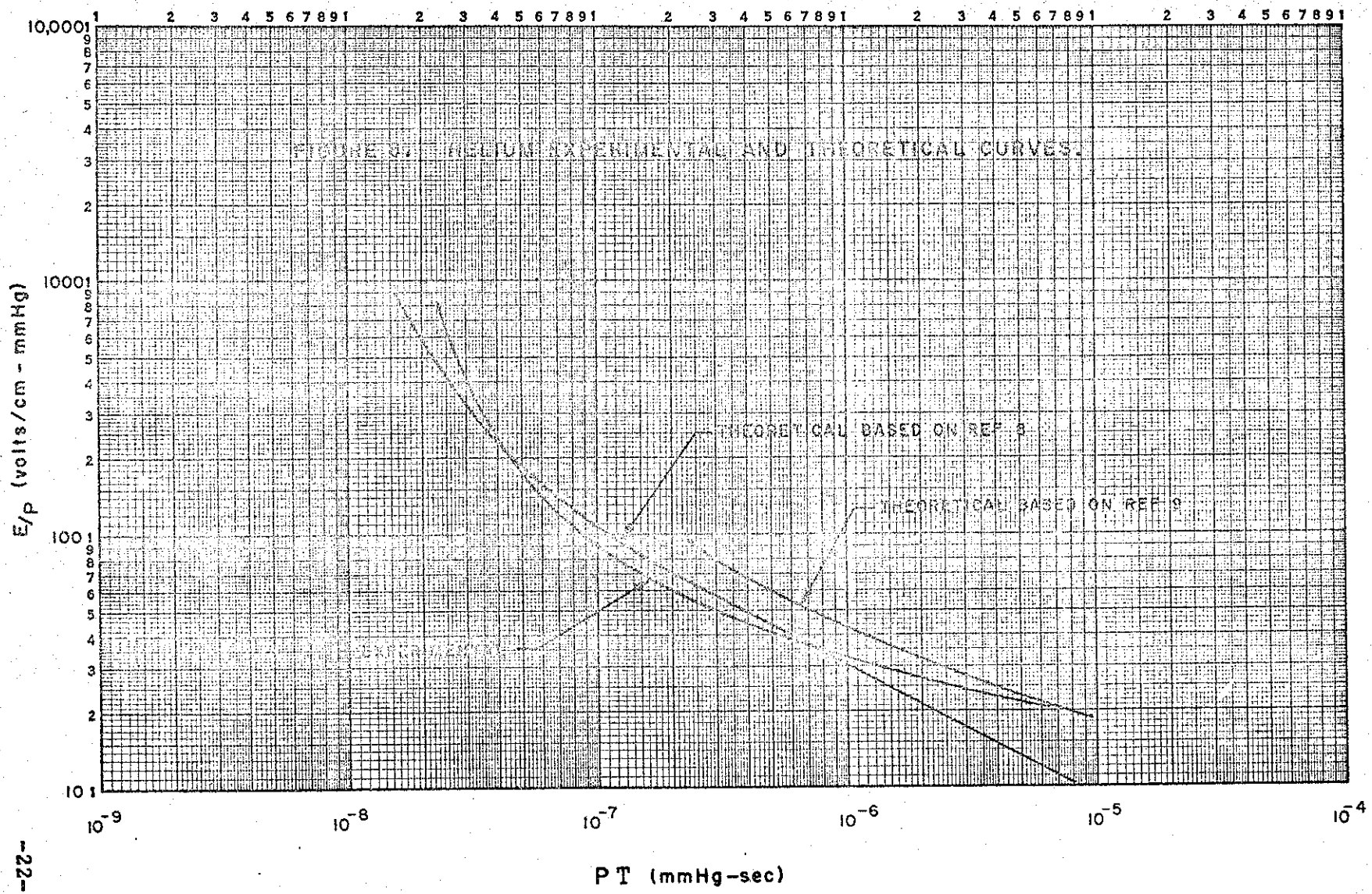

FIGURE 9. HELIUM EXPERIMENTAL AND THEORETICAL CURVES.

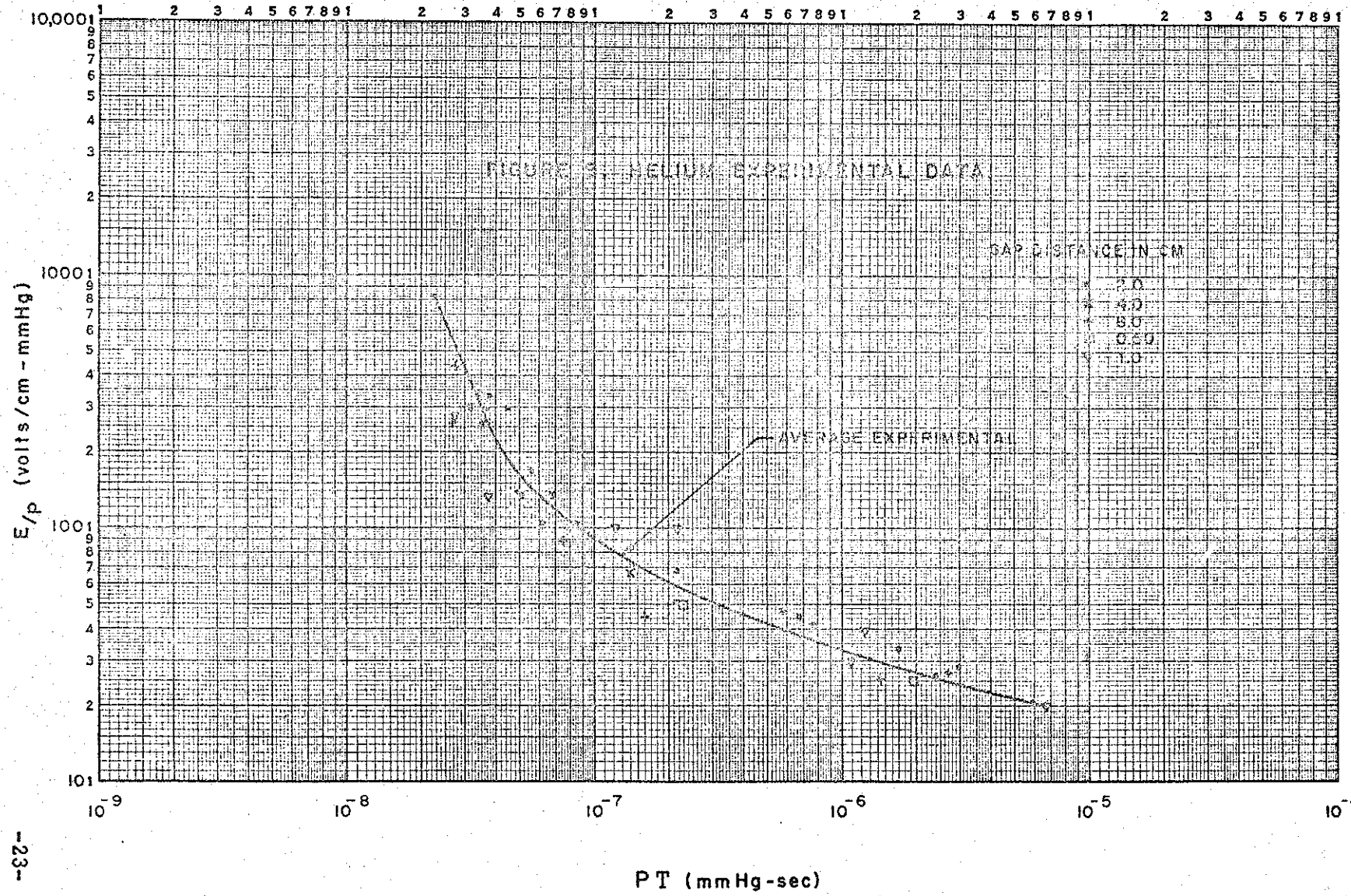
10,000
1000
100
10
E/p (volts/cm - mmHg)
10^{-9}
10^{-8}
10^{-7}
10^{-6}
10^{-5}
10^{-4}
PT (mmHg-sec)
GAP DISTANCE IN CM
2.0
3.0
5.0
7.0
10.0

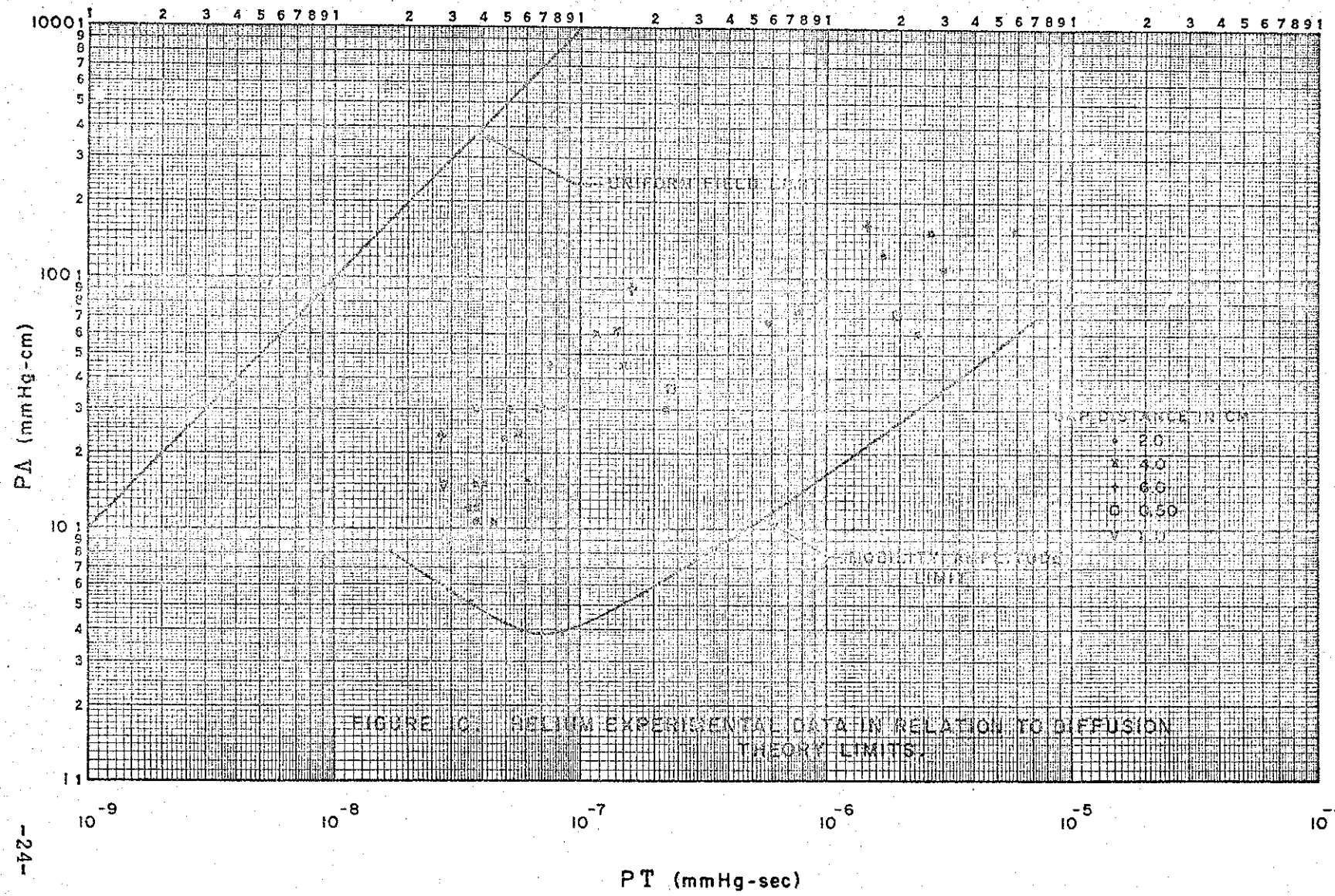

FIGURE 10. HELIUM EXPERIMENTAL DATA IN RELATION TO DIFFUSION THEORY LIMITS.

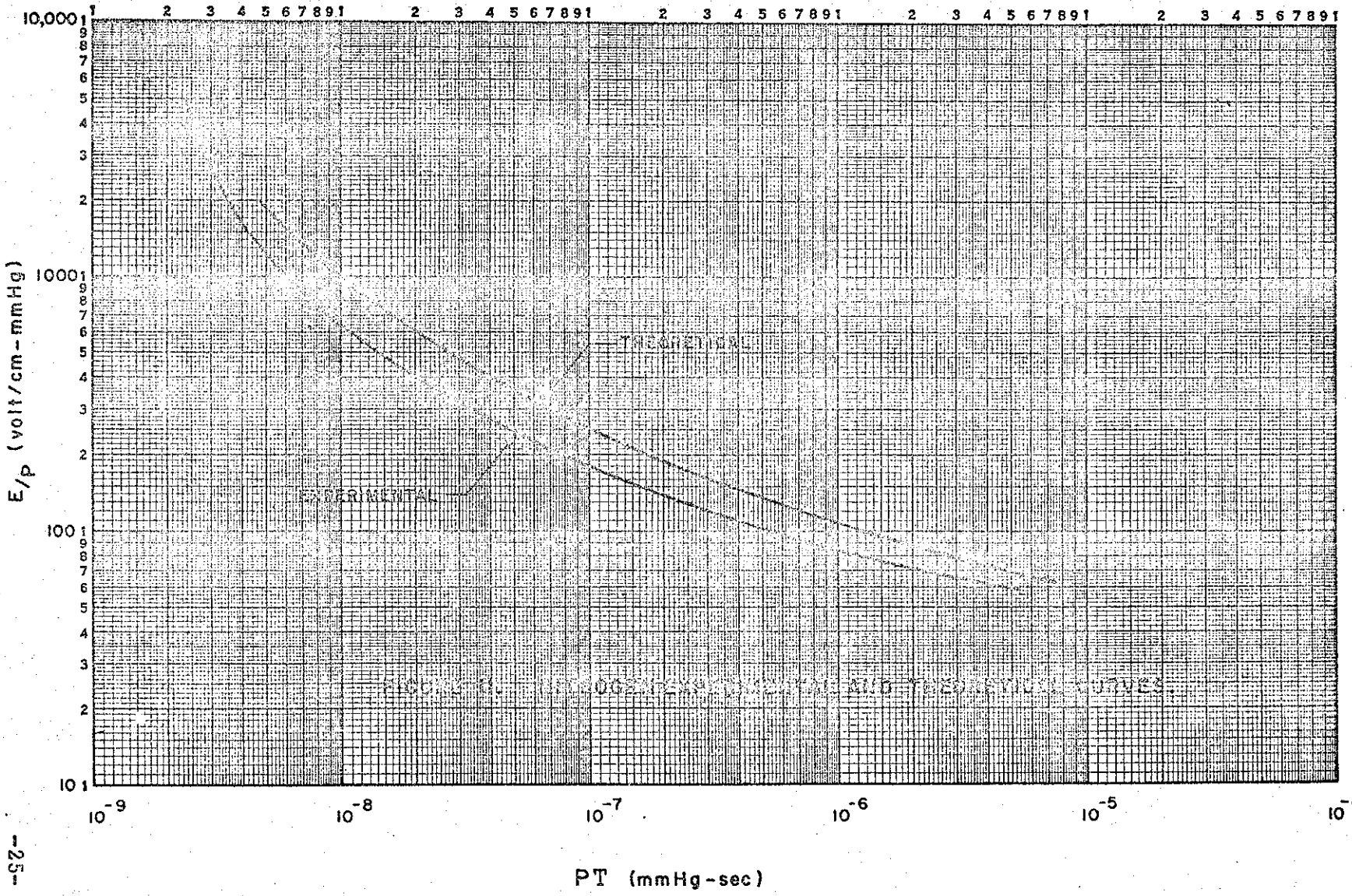
10,000
1000
100
10
E/p (volt/cm-mmHg)
EXPERIMENTAL
THEORETICAL
10^{-9}
10^{-8}
10^{-7}
10^{-6}
10^{-5}
10^{-4}
PT (mmHg-sec)

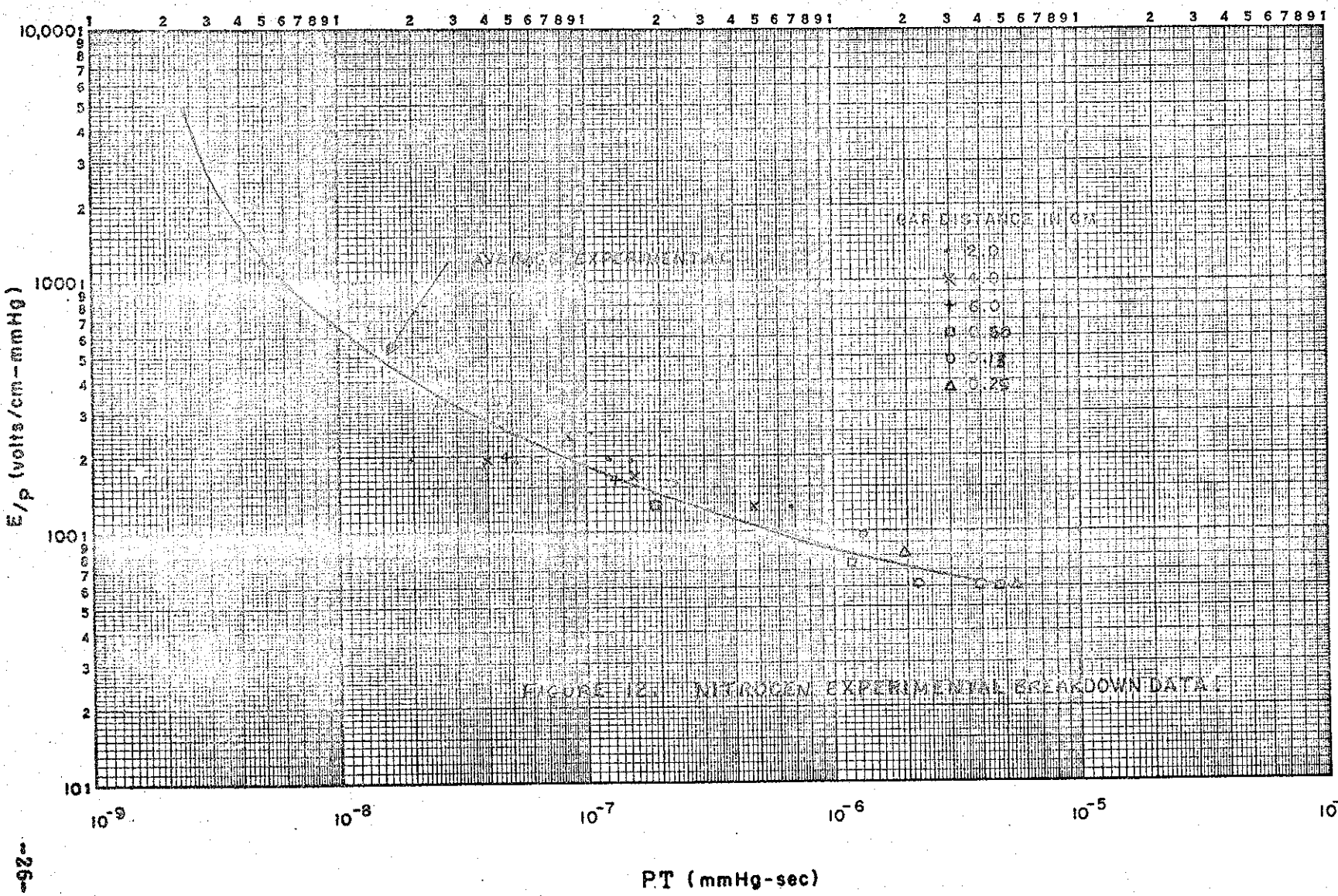

FIGURE 12: NITROGEN EXPERIMENTAL BREAKDOWN DATA.

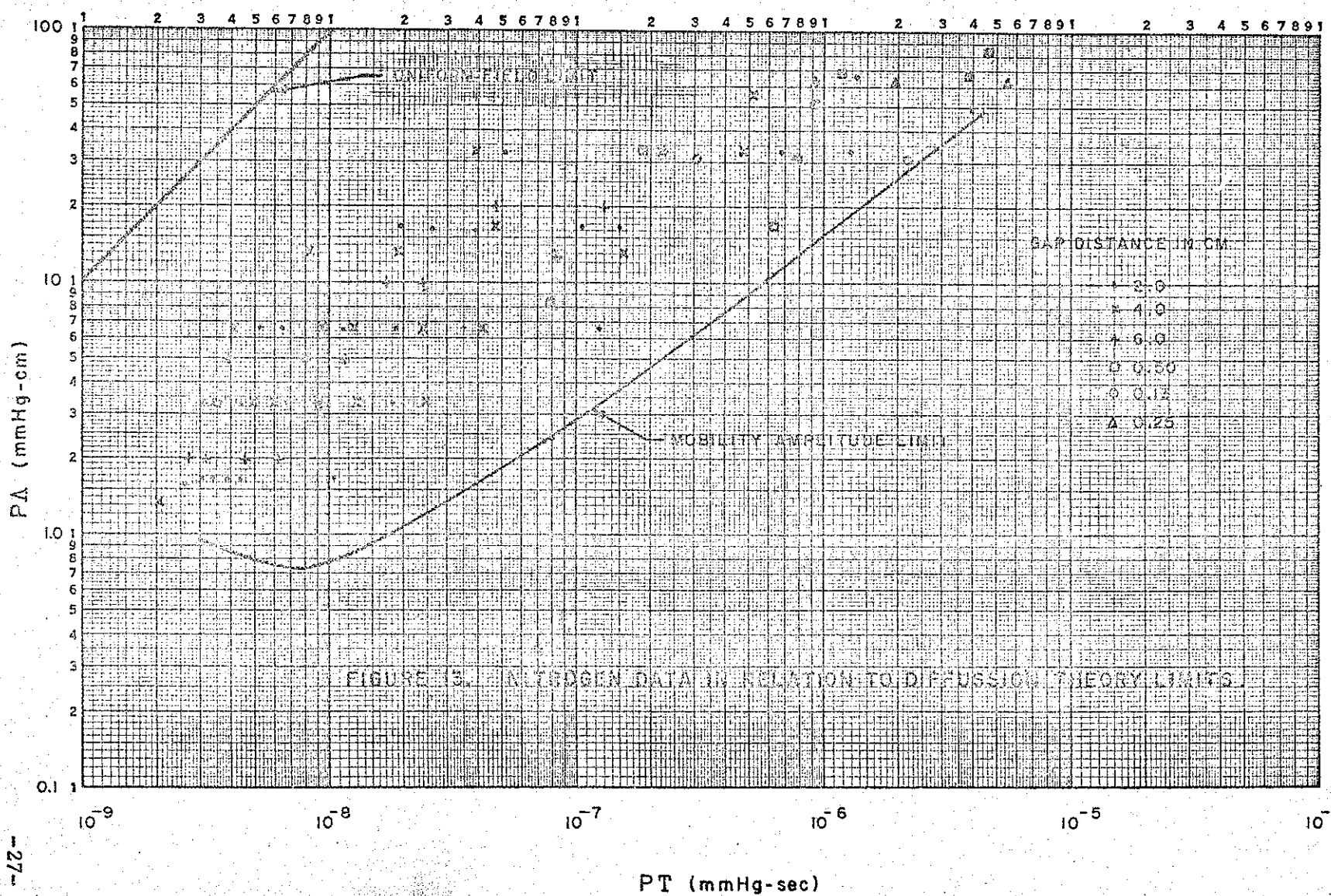

FIGURE 13. NEUTRON DATA IN RELATION TO DIFFUSION THEORY LIMITS